Check for updates

JGR Atmospheres

RESEARCH ARTICLE
10.1029/2020JD033534

Climatology of Near-Surface Daily Peak Wind Gusts Across Scandinavia: Observations and Model Simulations

Lorenzo Minola[1], Cesar Azorin-Molina[2], Jose A. Guijarro[3], Gangfeng Zhang[4,5], Seok-Woo Son[6], and Deliang Chen[1]

[1]Regional Climate Group, Department of Earth Sciences, University of Gothenburg, Gothenburg, Sweden, [2]Centro de Investigaciones sobre Desertificación, Consejo Superior de Investigaciones Científicas (CIDE-CSIC), Valencia, Spain, [3]State Meteorological Agency (AEMET), Delegation at the Balearic Islands, Palma de Mallorca, Spain, [4]State Key Laboratory of Earth Surface Processes and Resource Ecology, Beijing Normal University, Beijing, China, [5]Academy of Disaster Reduction and Emergency Management, Ministry of Civil Affairs and Ministry of Education, Beijing Normal University, Beijing, China, [6]School of Earth and Environmental Sciences, Seoul National University, Seoul, South Korea

Key Points:

- A daily wind peak gusts dataset is homogenized for 127 Scandinavian stations, which are classified as coastal, inland and mountainous
- Examined regional climate models improve daily peak wind gusts simulations over all regions when compared to their driving models
- The regional climate models do not have adequate skills in simulating daily peak wind gusts across inland and mountainous regions

Supporting Information:

Supporting Information may be found in the online version of this article.

Correspondence to:

D. Chen,
deliang@gvc.gu.se

Citation:

Minola, L., Azorin-Molina, C., Guijarro, J. A., Zhang, G., Son, S.-W., & Chen, D. (2021). Climatology of near-surface daily peak wind gusts across Scandinavia: Observations and model simulations. *Journal of Geophysical Research: Atmospheres*, *126*, e2020JD033534. https://doi.org/10.1029/2020JD033534

Received 15 JUL 2020
Accepted 18 FEB 2021

© 2021. The Authors.
This is an open access article under the terms of the Creative Commons Attribution-NonCommercial-NoDerivs License, which permits use and distribution in any medium, provided the original work is properly cited, the use is non-commercial and no modifications or adaptations are made.

Abstract An observed daily peak wind gusts (DPWG) dataset over Scandinavia, consisting of time series from 127 meteorological stations across Finland, Norway and Sweden, has been created. This dataset provides high-quality and homogenized near-surface DPWG series for Scandinavia, spanning the longest available time period (1996–2016). The aim of this study is to evaluate the ability of two regional climate models (RCMs) in simulating DPWG winds. According to the observed DPWG climatology, meteorological stations are classified into three regions for which wind conditions are influenced by similar physical processes: coast, inland and mountain. Smaller-scale DPWG features of the three regions are only captured when coarser general circulation models or reanalyses are downscaled by a RCM. Dynamic downscaling is thus needed to achieve more realistic simulations of DPWG when compared to their driving models. The performances of the RCMs are found to be more dependent on model dynamics and physics (such as gust parametrization) than on the boundary conditions provided by the driving models. We also found that the RCMs cannot accurately simulate observed DPWG in inland and mountainous areas, suggesting the need for higher horizontal resolution and/or better representation of relevant boundary-layer processes.

1. Introduction

Rising global air temperatures in the 21st century are driving changes in the hydrological and energy cycles (IPCC, 2014), as well as in other climate variables such as surface wind (Zeng et al., 2019). Climate change is manifested locally via more frequent and severe regional extreme weather and climate extremes, such as heat waves, heavy precipitation, droughts and floods (Beniston et al., 2007; Chen et al., 2020). Among those climate hazards, windstorms and extreme winds can seriously threaten human life, property, infrastructure and ecosystems by affecting aviation security, wind energy production and damaging buildings and forests (Suomi & Vihma, 2018). Across Europe, extreme wind events contribute to more than half of the economic losses associated with natural disasters (Ulbrich et al., 2013); during 1980–2017, windstorms accounted for 62% of the insured economic losses from climate-related extremes (EEA, 2019). In Scandinavian countries like Sweden and Finland, which are largely covered by forests, wind-induced damage significantly impacts timber production and thus the national economy (Gregow et al., 2017; Hannon Bradshaw, 2017; Peltola et al., 2010).

For monitoring the turbulent fluctuations of wind, WMO (1987) suggests recording and archiving the so-called near-surface (~10-m height) wind gusts, defined as the maximum of the 3 s running average wind speed over the time interval. Due to this short averaging time, wind gust measurements can capture the sudden and abrupt changes in wind that may exert extreme loads on buildings and structures. By having access to long-term, continuous and representative wind gust observations, extreme wind risk assessments and forecasting can be carried out (Suomi & Vihma, 2018). An increasing number of studies have investigated multidecadal changes of daily peak wind gusts (hereafter DPWG), defined as the highest wind gust recorded in 24 h (Azorin-Molina et al., 2016). However, high-quality and continuous DPWG measurements are often not available. For example, in Scandinavian countries, observed wind gust records are only available

since the mid-1990s, when automatic weather stations were introduced (see Section 2.1). Even when measurements are available, their quality can be poor as observed wind series can be strongly affected by various measurement inconsistencies (Aguilar et al., 2003), such as station relocation or anemometer height changes (Wan et al., 2010) and anemometer drift (Azorin-Molina et al., 2018a).

Reliable DPWG observations are not always accessible. Therefore, understanding how the changing climate affects extreme wind characteristics, including future wind gust scenarios, requires regional climate models (hereafter, RCMs). An RCM is a limited-domain climate model which, forced by lateral and ocean conditions from a general circulation model (GCM) or an observation-based data set (reanalysis), simulates climate variability with regional refinements (http://glossary.ametsoc.org/wiki/Regional_climate_model; last accessed February 16, 2021). This improved accuracy is enabled, for example, by the more detailed surface characteristics and higher-resolution topography. Because the RCM domain is limited, boundary values are provided by the coarser driving model (GCM or reanalysis). By downscaling global reanalyses or GCMs, information on the large-scale flow are included in the regional simulations at the lateral boundaries, while regional, small-scale circulation features are generated by the RCM. Therefore, RCMs enable more detailed study not only of the mean conditions, but also extremes (Beniston et al., 2007), by running climate simulations at higher resolution in both time and space (typically at horizontal scales of 10–50 km) than the GCMs. Moreover, wind gust outputs are available in current RCMs. However, climate models can only explicitly resolve processes whose scales of motion are greater than the model grid scale. Therefore, the cumulative effects of all the eddies responsible for gusts must be related to those variables and processes occurring at the resolvable scales of the model: this approach is named parametrization (Anthes, 1985). Current RCMs parametrize wind gustiness using various techniques (Sheridan, 2011) and can quantify possible changes in wind extreme statistics under different future scenarios (Jeong & Sushama, 2019; Nikulin et al., 2010), thus providing a primary tool for the development of risk management strategy or adaptation policy. However, before any RCM product can be used to assess changes in extreme winds, its ability in representing observed near-surface wind statistics (such as gusts) must be proven. Following the work by Kunz et al. (2010) for Germany, the capability of RCMs in realistically simulating gust wind speeds must be investigated using observations. Unfortunately, there are currently no suitable DPWG observational datasets for Scandinavia which can be used to verify wind model outputs (Nikulin et al., 2010), and the reliability of available RCMs in simulating wind remains largely unknown (Achberger et al., 2006).

To fill such gaps, this work aims to: (i) create the first high-quality and homogenized near-surface DPWG dataset for the Scandinavian Peninsula (i.e., Finland, Norway and Sweden) by applying a robust homogenization protocol; (ii) improve our understanding of the observed spatiotemporal DPWG climatology across Scandinavia for 1996–2016; and (iii) evaluate the performance of RCMs in simulating DPWG by comparison against the observations. We note that it is beyond the scope of this study to exhaustively analyze all possible RCMs available across Scandinavia. Instead, by selecting a few RCMs and comparing their outputs with observed DPWG series, this study aims to reveal new insights into regional wind gust climate simulations by identifying: (i) the observed features missed by current RCMs; (ii) the advantages of RCM downscaling compared to GCMs; and (iii) the factors in the RCM setup which affect the model performance in simulating DPWG the most (e.g., lateral boundary conditions, wind gust parametrization, etc.).

2. Data

2.1. Observed DPWG

Hourly wind gust observations across Finland, Norway and Sweden are used to create the first quality-controlled and homogenized DPWG dataset for Scandinavia.

Wind gust observations across Finland are provided by the Finnish Meteorological Institute (FMI; https://en.ilmatieteenlaitos.fi/climate-statistics; last accessed February 16, 2021). FMI measures wind gust as maximum 3-s wind speed, following WMO (2014) guidelines. FMI greatly increased the number of automatic weather stations at the end of the 1990s, and there were fewer wind gust observations before this time (J.-P. Kaukoranta, 2020; personal communication). Meteorological stations use a Vaisala WA15 anemometer and Adolf Thies GmbH & Co. KG ultrasonic anemometer 2D wind measurements (M. Santanen, 2019; personal

communication). Since the mid-1990s, most of the WA15 anemometers have been changed to Thies ultrasonic anemometers, but many WA15 instruments are still in use.

In Norway, wind gust is measured by the Norwegian Meteorological Institute (MET Norway) and hourly observations can be downloaded at the eKlima web portal (http://sharki.oslo.dnmi.no/portal/page?_pageid=73,39035,73_39049&_dad=portal&_schema=PORTAL; last accessed February 16, 2021). For MET Norway weather stations, wind gust is defined as the maximum 3-s wind speed in the last hour, following the WMO (2014) output-averaged time instructions (R. G. Skaland, 2020; personal communication). Similar to Finland, fewer wind gust data are available across Norway before 1996, since the number of automatic weather stations began to increase rapidly at the end of the 1990s. Both Gill Wind Observer II and Young Wind Monitor-MA anemometers have been adopted to measure near-surface wind by MET Norway, with a few stations still equipped with Vaisala WAV151 instruments (H. T. Husebye, 2019; personal communication).

Hourly wind gust measurements across Sweden are provided by the Swedish Meteorological and Hydrological Institute (SMHI) through its open data page (https://www.smhi.se/data/utforskaren-oppna-data/; last accessed February 16, 2021). Wind gusts were measured at 10-m height as the maximum 2 s gust recorded in the last hour (S. Lekander, 2019; personal communication), which differs by 1 s from the standard 3 s averaging time suggested by WMO (2014) and followed in records across both Finland and Norway. Similar to FMI and MET Norway, SMHI started to install automatic weather stations across the country in 1996: for this reason, systematic wind gust measurements are available only since the end of the 1990s (Wern & Bärring, 2009). Automatic weather stations across Sweden are equipped with Thies 2D ultrasonic anemometers.

Using the hourly measurements, DPWG series were calculated by selecting the maximum wind gust record for each day when more than 20 measurements were available during the 24 h. A total of 127 meteorological stations, comprising 17 stations in Finland, 20 in Norway and 90 in Sweden, are considered for the period 1996–2016. These stations are chosen because they cover the longest available time period of observations across Finland, Norway and Sweden with less than a year of missing data (i.e., <365 days when the DPWG could not have been calculated).

2.2. Simulated DPWG

This study uses wind gust outputs from two RCMs downscaled in the Coordinated Regional Downscaling Experiment (CORDEX, Giorgi et al., 2009): (i) RCA4, the RCM developed by the Rossby Center, which is part of SMHI (Strandberg et al., 2014); and (ii) RACMO22E, which is version 2 for Europe of the KNMI (Royal Netherlands Meteorological Institute) regional atmospheric climate model (RACMO2; van Meijgaard et al., 2012). Across Europe (in the so-called Euro-CORDEX experiments), each RCM model provides data on a horizontal spacing of 0.11° (~12.5 km) in a rotated latitude-longitude grid. The RCMs examined in this study are driven by boundary conditions from the reanalysis ERA-Interim (hereafter, ERAINT) product of the European Center for Medium-Range Weather Forecasts (ECMWF; Dee et al., 2011), and two different GCMs: ICHEC-EC-EARTH (hereafter, ICHEC) and MOHC-HadGEM2-ES (hereafter, MOHC) from the fifth phase of the Coupled Model Intercomparison Project (CMIP5; Taylor et al., 2012). When downscaled using ERAINT, wind gust simulations cover the time period ~1980–2010; with the ICHEC and MOHC boundary conditions, outputs are available for a ~1950–2005 control run ("historical") under present-day climate conditions and for various 2005–2100 scenario simulations based on the different radiative forcing stabilization levels by 2100 (the so-called representative concentration pathways, RCPs). Table 1 summarizes the RCMs used in this study and more information about the CORDEX models may be found at https://cordex.org/?option=com_content&view=article&id=242&Itemid=769 (last accessed February 16, 2021).

Among the different RCMs available in Euro-CORDEX, RCA4 and RACMO22E have been chosen because: (i) both models have been run with same boundary conditions (ERAINT, ICHEC and MOHC); and (ii) wind gusts are calculated in each RCM using a different gust parametrization. Following Brasseur (2001), RCA4 estimates wind gusts by considering the deflection of air parcels traveling at a given height, which are able to reach the surface when the mean turbulent kinetic energy of large turbulent eddies is greater than the buoyant energy difference between the surface and the height of the parcel. In contrast, RACMO22E

Table 1
Details of the CORDEX RCMs chosen in this study

RCM name	Driving model	Abbreviation	Experiment	Ensemble	RCM version	Time period	Calendar	Domain	Institute	Reference
RCA4	ERAINT	RCA4-ERAINT	Evaluation	r1i1p1	v1	1980–2010	Standard	EUR-11	SMHI	Strandberg et al. (2014)
	ICHEC-EC-EARTH	RCA4-ICHEC	Historical	r12i1p1	v1	1951–2005	Standard			
	MOHC-HadGem2-ES	RCA4-MOHC	Historical	r1i1p1	v1	1951–2005	360 days			
RACMO22E	ERAINT	RACMO22E-ERAINT	Evaluation	r1i1p1	v1	1979–2012	Standard	EUR-11	KNMI	van Meijgaard et al. (2012)
	ICHEC-EC-EARTH	RACMO22E-ICHEC	Historical	r12i1p1	v1	1950–2005	Standard			
	MOHC-HadGem2-ES	RACMO22E-MOHC	Historical	r1i1p1	v2	1950–2005	360 days			

calculates wind gust as the sum of: (i) 10-m wind speed; (ii) turbulent gustiness expressed as a function of the shear-stress and the boundary layer stability; and (iii) a contribution from deep convection in strong wind-shear environments such as frontal systems (Bechtold & Bidlot, 2009; Panofsky et al., 1977). RCA4 has 40 vertical levels with a model time step of 450 s (G. Nikulin, 2021; personal communication). RACMO22E has 40 vertical levels (Kotlarski et al., 2014) and time step of 2 min (Lenaerts et al., 2014). Both RCA4 and RACMO22E use the Gtopo30 database to represent the land topography and for each grid cell they integrate the dataset as piecewise constant (Samuelsson et al., 2015; Undén et al., 2002).

To evaluate the added value of using a high-resolution RCM, the wind gust outputs of the driving data (ERAINT) are compared to the wind gusts of its downscaled regional model (RCA4-ERAINT or RACMO22E-ERAINT). The ERAINT reanalysis provides a coherent and spatially complete record of the global atmospheric circulation, by assimilating information from different types and sources of observations into a forecast model (Dee et al., 2011). A realistic model is used to extrapolate information from locally observed variables to unobserved parameters at nearby locations (spatial completeness), while the laws of physics of the forecast model as well as the observations guarantee the physical coherency of the estimated variables. Due to the completeness and physical coherence, as well as the quality of the reanalyzed fields, ERAINT is the dataset which provides the best lateral boundary conditions (so-called "perfect boundary conditions") for the downscaling of the studied RCMs (Giorgi et al., 2009; Strandberg et al., 2014). Three-hourly wind gust outputs are available for ERAINT at its horizontal resolution of 80 km. Similar to RACMO22E, ERAINT computes gusts following the parametrization of Panofsky et al. (1977) and Bechtold and Bidlot (2009) (for detailed information about the ERAINT gust parametrization, see ECMWF, 2007).

Simulated DPWG series are constructed by selecting the maximum wind gust output at each grid point for each day in the different model datasets (ERAINT and the different RCMs). For model evaluation, the observed DPWG time series at a given station are compared with the estimated DPWG at the closest model (reanalysis or RCM) grid point, assuming that the closest series matches the observed one better than any other more distant grid point series (Minola et al., 2020). DPWG simulations are compared with observations during 1996–2005, i.e. the common time period available for both data sets during only the RCM "historical" experiment.

3. Study Region

The topographic features of the Scandinavian Peninsula (Finland, Norway and Sweden) are shown in Figure 1. The Scandes mountain range crosses the west side of the Peninsula in a north-to-south-direction. The Scandes are mainly located in Norway, where they dominate the landscape, reaching approximately 2,500 m above sea level at the highest elevations. The coastline is characterized by fjords, i.e. narrow inlets with steep sides created by glacial erosion. The Scandes are also the main topographical feature in central and northern Sweden, while southern Sweden is mostly flat with only few elevated areas of minor extent

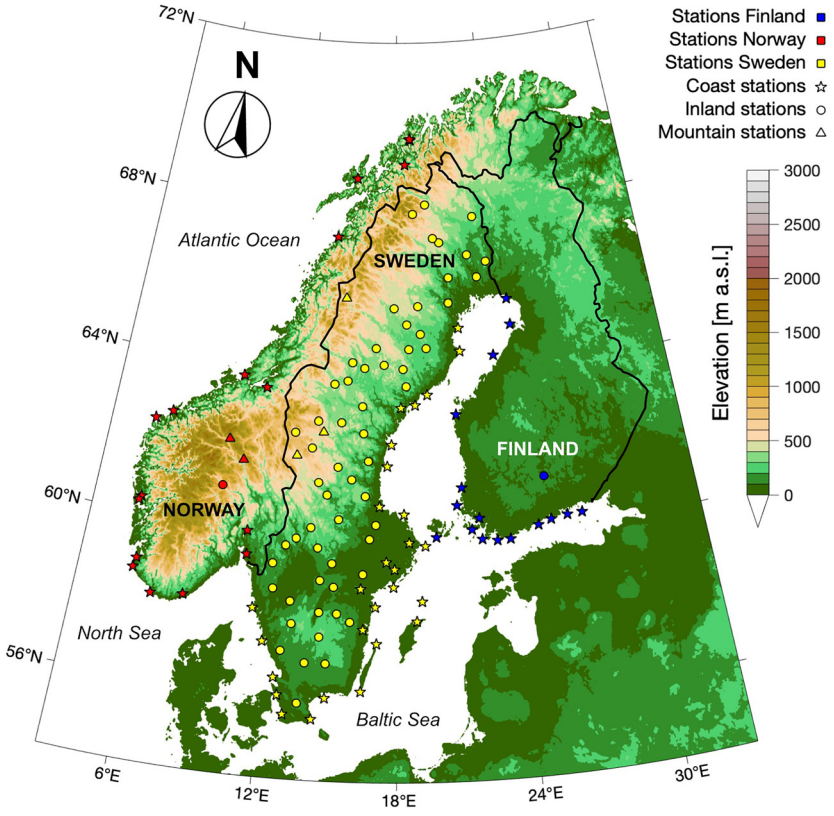

Figure 1. Map of the study area showing topography and the location of the 17 weather stations across Finland (blue), 20 stations across Norway (red) and 90 stations across Sweden (yellow). Coastal stations are shown as stars, inland stations as circles, mountain stations as triangles.

(Achberger et al., 2006). Similar to southern Sweden, the topography of Finland is gentle and mostly flat, marked with many lakes and low hills.

The locations of the selected 127 weather stations are displayed in Figure 1. The map shows how the selected stations are able to evenly cover the whole of Sweden, in both coastal and inland regions. However, most of the chosen Finnish and Norwegian weather stations are located along the coast, except of 1 station (out of 17) in Finland and 3 stations (out of 20) in Norway which are located further than 20 km from the shoreline.

4. Methods

4.1. Homogenization

Various types of nonclimatic factors, such as station relocations and anemometer height and type changes (Wan et al., 2010), can affect near-surface wind series, making those data unrepresentative of the actual climate and its variations over time (Aguilar et al., 2003). A homogenization protocol must then be applied to identify artificial shifts (or break-points) and afterward remove the biases which those inhomogeneities create. Here, *Climatol* (Guijarro, 2017) is used to perform homogenization and missing data infilling on the raw DPWG series. *Climatol* is a R (R Core Team, 2020) package designed for quality controlling, homogenizing and infilling climate series. The package can be installed from a R running session or downloaded from https://CRAN.R-project.org/package=climatol (last accessed February 16, 2021). Further information are available at http://www.climatol.eu/ (last accessed February 16, 2021). *Climatol* has been widely and successfully applied to homogenize wind series in previous studies (e.g., Shi et al., 2019; Zhang et al., 2020) and also to homogenize DPWG (Azorin-Molina et al., 2016, 2019). For this reason, it was chosen here to perform the homogenization of DPWG series across Scandinavia. By working with "normalized" values (here, normalization of a time series is achieved through division by the series average), *Climatol* performs

homogenization using a two-step iterative approach (Guijarro, 2018). In step 1, the DPWG series are calculated by averaging their five closest series at each time step, and break-points are identified by applying the well-established standard normal homogeneity test (SNHT; Alexandersson, 1986) to the differences between the observed and the calculated "normalized" values, at two different stages: (i) on stepped overlapping time windows, to minimize the possible masking effect of multiple break-points; and (ii) on the whole series. Break-point finding is repeated iteratively until no SNHT values higher than the specified thresholds (150 for the stepped window and 100 when applied to the complete series) are detected. The values of the SNHT thresholds were chosen through exploratory homogenizations run by *Climatol*. In step 2, once all break-points are identified and corrected, missing values are filled by means of the five closest observations, weighted by an inverse distance function. Notice that: (i) to avoid the rejection of actual extreme values, no threshold of outlier tolerance is set, at the cost of allowing erroneous values to be accepted; and (ii) the closest series (reference series), needed both for finding break-points and for infilling of missing values, were chosen only among those measured by the same meteorological institute, to avoid differences in measuring procedures between the various institutes (such as different gust duration definitions: see Section 2.1) which could affect the homogenization. A total of 59 time steps were missing in all DPWG series across Sweden for which *Climatol* could not complete the homogenization because a complete reference series was needed. For this reason, those 59 days of missing observations were filled before *Climatol* was applied by using the 1996–2016 daily means. Notice that the applied relative homogenization (i.e., comparison with the five closest stations) cannot remove systematic biases present in the whole time series. For example, if one station is located at a height different than 10 m, such bias cannot be detected and removed. In the same way, the relative homogenization cannot deal with those biases produced (near)simultaneously in most or all the series (such as a sensor change in all the stations of the network).

4.2. Statistics for Comparison

To evaluate the similarity in mean DPWG simulated using the same RCM model or under the same boundary conditions (see Section 5.3), a scatterplot of two data sets X and Y (created by using different model setups, i.e. RCM + boundary condition) is plotted and the agreement is quantified through the coefficient of determination R^2 (Von Storch & Zwiers, 1999). Under the hypothesis Y = X (the two data sets are equal), R^2 quantifies the ability of such linear regression to explain the variation of the data in the scatterplot: R^2 values closer to 1 indicate that stations in Y are more closely associated to stations in X throughout their mean DPWG values.

4.3. Regionalization of DPWG Series

Topographic features are known to influence the surface energy balance and, especially over mountainous terrain, the thermally and dynamically forced earth-atmosphere exchange processes shape the atmospheric boundary layer (ABL) through turbulent transport (Helbig et al., 2017; Rotach et al., 2016). The resulting inhomogeneous ABL drives mesoscale and even sub-mesoscale flows (e.g., slope and valley winds), which strongly affect regional wind characteristics. Figure 2 shows the mean and standard deviation of DPWG at each weather station for 1996–2016 plotted against the station's distance to the sea and its elevation. Stations tend to group into three clusters: (i) stations close to the coast are characterized by high mean and standard deviation; (ii) stations in high-elevation areas also show high mean and standard deviation; and (iii) stations at low elevation or in inland regions show low mean and standard deviation. Based on these characteristics, we classify meteorological stations across Scandinavia into three groups: (i) coast stations, within 20 km of the sea; (ii) inland stations, which are located further than 20 km from the coast and at an elevation below 750 m above sea level (a.s.l.); and (iii) mountain stations, with elevations higher than 750 m a.s.l. Similar regionalization groups have been adopted in previous studies (see Azorin-Molina et al., 2018b). Grouping stations into coastal, inland and mountain regions particularly enables explanations of potential differences and similarities in DPWG statistics according to common regional physical processes. At coastal stations, wind conditions are mainly governed by local differences between sea and land (e.g., differences in heat capacity, surface roughness, the associated ABL turbulence; Achberger et al., 2006; Borne et al., 1998). Coastal wind conditions are also affected by synoptic-scale systems such as extratropical cyclones and storms (Feser et al., 2015). At inland stations, winds are strongly affected by earth-atmosphere interaction through

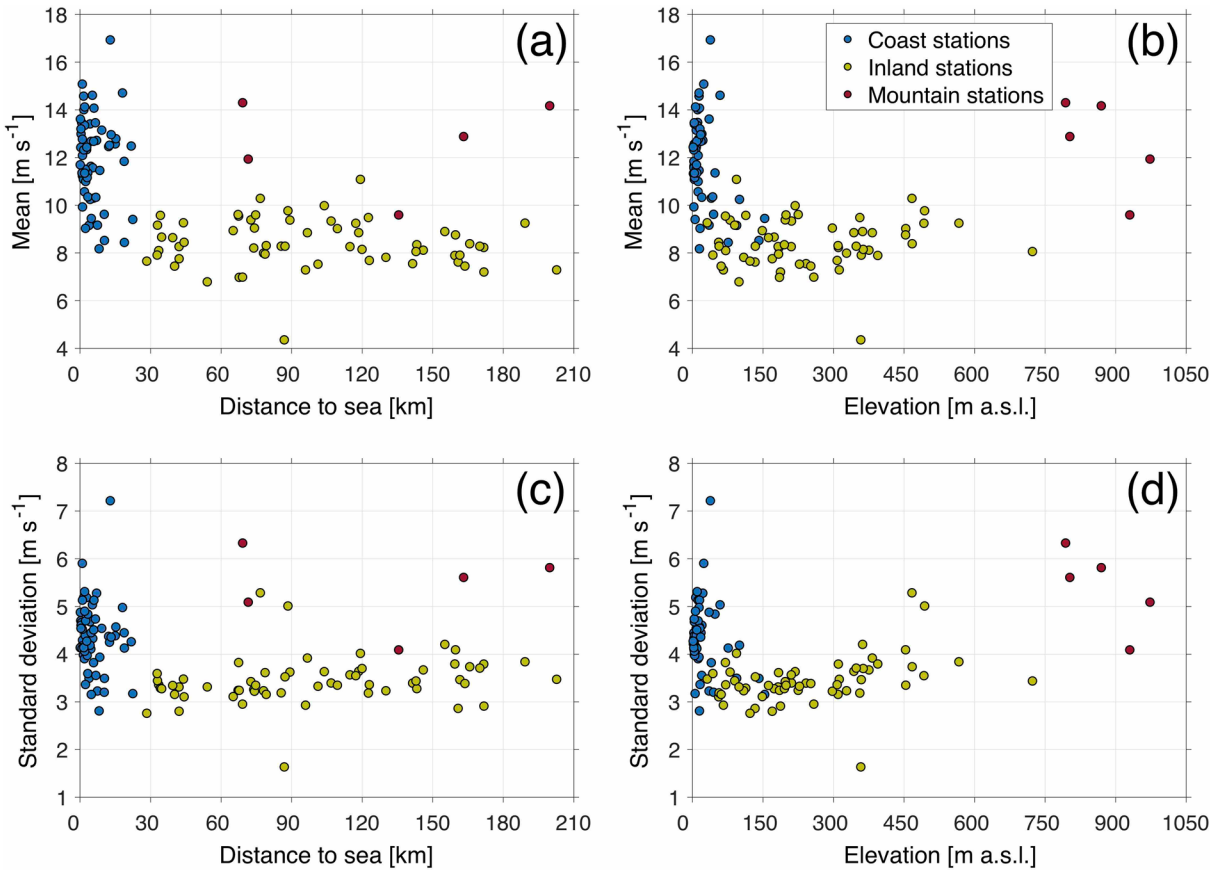

Figure 2. Scatterplot of the mean (top row) and standard deviation (bottom row) of daily peak wind gusts for the 127 homogenized stations across Scandinavia for 1996–2016 plotted against station distance to the sea (left) and elevation (right). Scatter-points cluster into three groups: (i) coastal stations (blue), (ii) inland stations (olive) and (iii) mountain stations (brown).

turbulent transport, driven, for example, by friction and heat exchange (Rotach et al., 2016). At upland stations, complex topography favors the development of local wind systems which are often suppressed by stronger larger-scale winds in the free troposphere (Achberger et al., 2006; Rotach et al., 2016; Serafin et al., 2018). This classification is also used when presenting results in the following sections, helping to overcome the issue of the uneven distribution of stations across Scandinavia (e.g., results could be dominated by a greater number of stations located in a particular region; Räisänen et al., 2003).

5. Results

5.1. Climatology of Observed DPWG

Figure 3 shows the spatial distribution of annual and seasonal mean and standard deviation of observed DPWG for 1996–2016. Annually, coastal stations generally display higher mean DPWG (greater than 10 m s^{-1}) than the inland stations (~8 m s^{-1}), except for a few stations located at high elevation in the Scandes range (~12 m s^{-1}). Seasonally, coastal stations show higher mean DPWG during winter and autumn when compared to spring and summer. This seasonality is different for inland stations, where only small differences are detected; however, slightly higher mean DPWG values are recorded during the warmer seasons (spring and summer) compared to the cooler months (winter and autumn). Again, just a few stations located in the high regions of the Scandes show strong seasonal-dependent signals similar to those of coastal stations. The spatial pattern of standard deviation of observed DPWG for 1996–2016 is similar to that just described for the mean. Stations located along the coast or in the higher-elevation areas of the Scandes show larger standard deviations than those of inland stations, and standard deviations are generally greater during cold months (winter) than warmer months (summer). When looking at the coefficient of variation

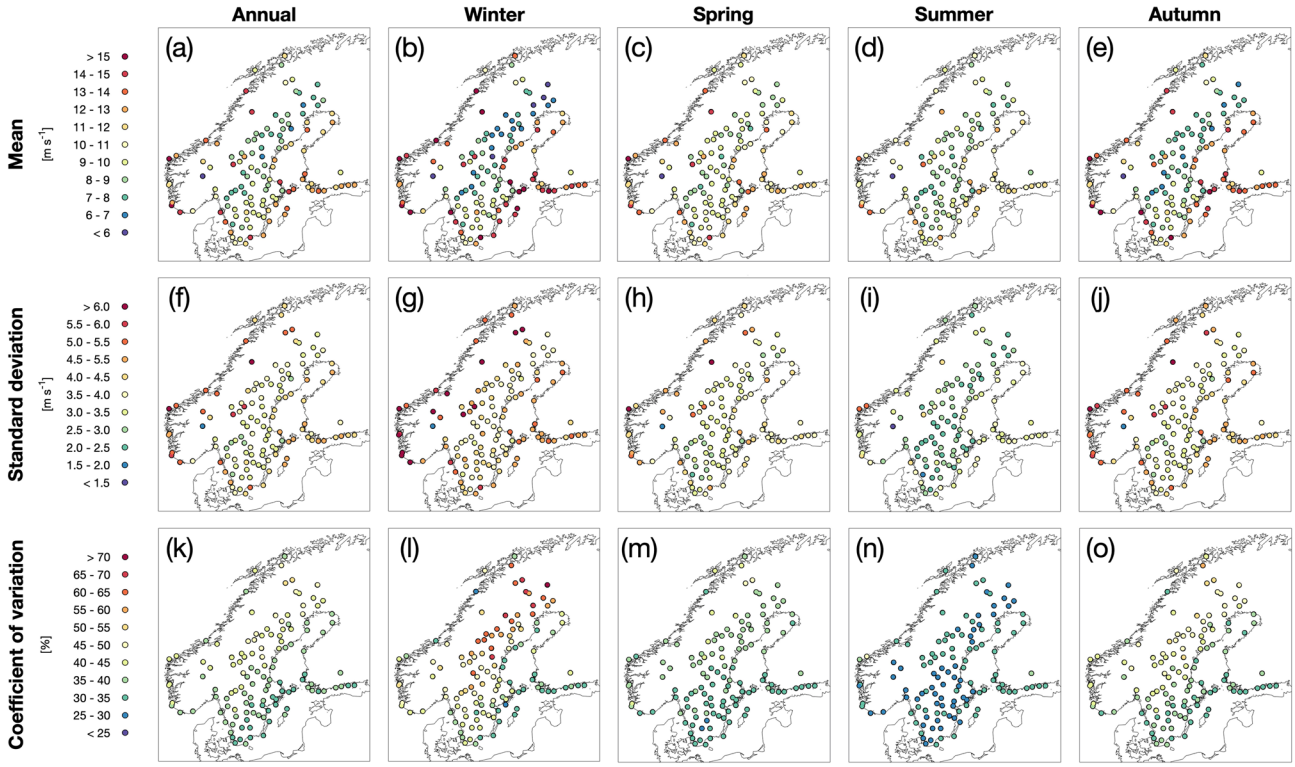

Figure 3. Annual and seasonal spatial distribution of the mean (a–e), standard deviation (f–j) and coefficient of variation (k–o) of the observed daily peak wind gusts for the 127 homogenized stations across Scandinavia for 1996–2016.

(i.e., the ratio between standard deviation and mean), inland stations, especially at latitudes higher than ~60°, show higher values compared to coast stations, in particular during winter.

The spatial differences identified in Figure 3 are better captured when stations are grouped into the three regions, with climate statistics displayed by region. For example, Figure 4 shows the seasonal cycle of mean and standard deviation of DPWG during 1996–2016 for each region. In coastal stations, the observed seasonal cycle of mean DPWG show the strongest winds in winter and the weakest winds in summer. The standard deviation also varies from month to month, ranging from ~5 m s^{-1} in December to ~3 m s^{-1} in July. In contrast, inland stations have a less pronounced seasonal cycle, with mean winds peaking in May-June at ~9 m s^{-1} similar to the average ~8 m s^{-1} recorded during the rest of the year. Standard deviation shows a seasonal signal similar to that of the coastal stations (higher during winter than summer), but with generally lower values (~4 m s^{-1} in December and ~2.5 m s^{-1} in July for the inland stations compared to ~5 and ~3 m s^{-1} for the coastal stations). For the mountain stations, observed DPWG also shows a seasonal cycle similar to that of the coastal stations, with the maximum and minimum values during the cold and warm months, respectively. The amplitude of the mean seasonal cycle in mountain regions is lower compared to coastal areas, and mountain stations generally show higher mean DPWG conditions for all months. The standard deviation of DPWG varies greatly during the year, reaching ~7 m s^{-1} in December, which is twice that during July (~3.5 m s^{-1}). Regional differences in the seasonal cycle can to a large extent be explained by the atmospheric stability (Achberger et al., 2006), although other factors such as topographical features also play a role. In fact, due to the larger heat capacity of water compared to land, stability over sea varies less than over land. The less stable atmosphere over water favors downward mixing of momentum over the sea and at coastal locations: this, together with the stronger pressure gradient in winter, enhances DPWG. Instead, the more stable conditions over land limit downward mixing of momentum in winter, thus reducing the seasonal DPWG variations.

It is evident from Figures 3 and 4 that, although there are differences in how wind gust is recorded across the different countries (3 s gust duration in Finland and Norway, but 2 s in Sweden; see Section 2.1), this

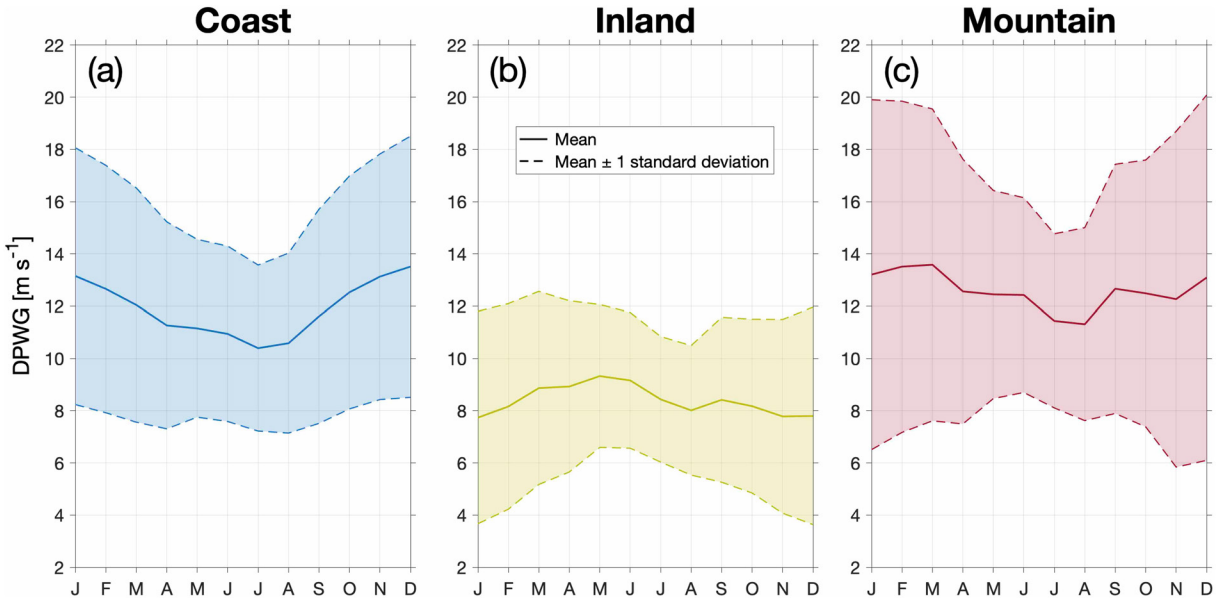

Figure 4. Mean seasonal cycle of daily peak wind gusts for stations in the coastal (left), inland (middle) and mountain (right) regions averaged for 1996–2016. The seasonal cycle is displayed as its mean value (solid line) and the standard deviation (colored area bounded by the dashed line).

does not seem to affect DPWG statistics across different countries. Specifically, stations located in the same region, but in different countries, show similar statistics in their DPWG conditions and do not greatly differ in their distribution (see example in Figure S1).

5.2. RCMs vs. Driving Models

To investigate if the RCM downscaling adds value to DPWG simulations compared to GCMs, the spatial distribution of mean DPWG for 1996–2005 is plotted in Figure 5 for observations, ERAINT and the two RCMs having ERAINT as their boundary conditions (RCA4-ERAINT and RACMO22E-ERAINT). Despite a ~80-km spatial resolution, ERAINT is able to capture the land-sea contrast and the impact of large-scale circulations with high DPWG in coastal regions as in the observations. The two RCMs also show high mean DPWG along the coastlines. However, while the simulated DPWG mean conditions vary according to the terrain features in both RCA4 and RACMO22E, the coarser horizontal resolution in ERAINT cannot resolve differences in DPWG climatology across inland regions, especially in the Scandes. An improved DPWG distribution in the RCMs is more evident in Figure 6 where mean DPWG values at each station are plotted as a function of the station's distance to the sea or its elevation for the ERAINT, RCA4-ERAINT and RACMO22E-ERAINT datasets. Again, high mean wind conditions at the coastal stations are captured by both ERAINT and RCMs. However, when looking at inland stations, ERAINT does not show distinct differences between high-elevation stations and other inland stations, even though both observations and RCMs show different wind conditions at stations with higher elevation. This discrepancy is likely caused by the fact that the horizontal spatial resolution of ERAINT (~80 km) is too coarse to capture the complex terrain features responsible for the gustiness and modified flow (Rotach et al., 2016). RCM simulations, with their higher horizontal resolution, are needed if the features most relevant for explaining the DPWG climatology across Scandinavia should be included.

We further evaluate potential discrepancies in modeled DPWG climatology between different RCMs with the same boundary condition or between the same RCM with different boundary conditions. Figure 7 presents the coefficient of variation (R^2) in scatterplots of mean DPWG for such cases. The R^2 values between RCA4 and RACMO22E are about 0.57 with a negligible sensitivity to the choice of boundary conditions (Figure 8a). In Figures 8b and 8c, R^2 values are further computed for the same RCM (RCA4 and RACMO22E, respectively) with different boundary conditions. In all simulations, R^2 is greater than 0.96. This result indicates that mean DPWG at a given station can vary widely when modeled by different RCMs even

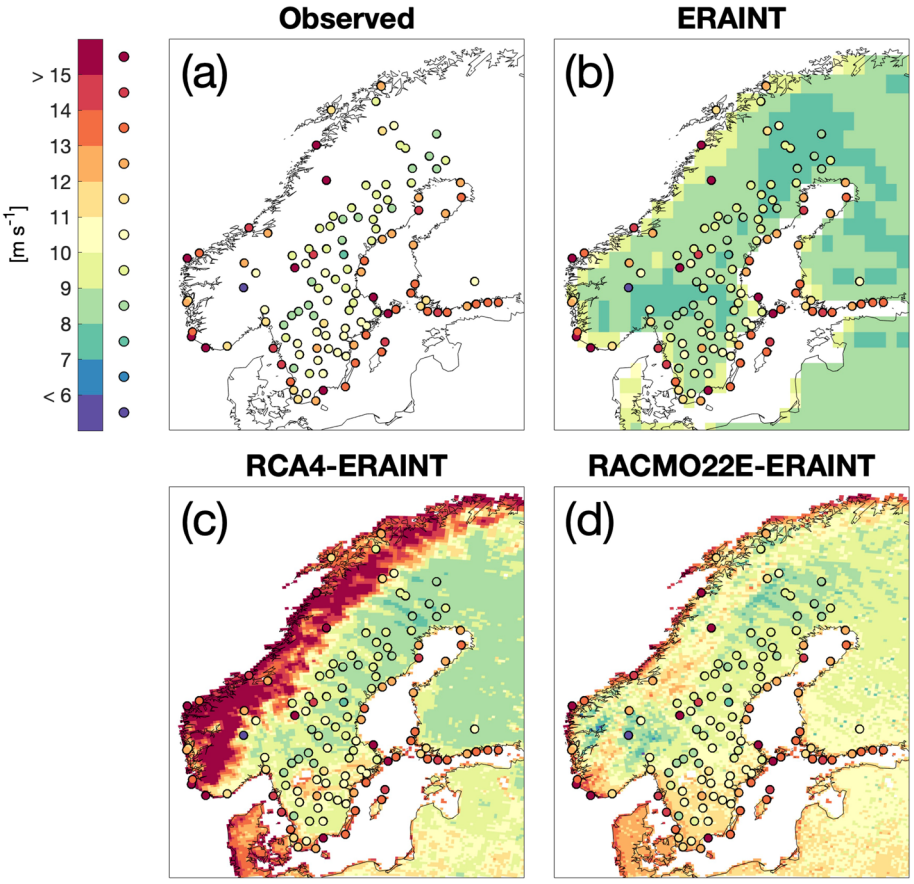

Figure 5. Spatial distribution of the annual-mean daily peak wind gusts calculated for 1996–2005 using observations (top-left), ERAINT (top-right), RCA4-ERAINT (bottom-left) and RACMO22E-ERAINT (bottom-right) datasets.

with same boundary conditions. The sensitivity of DPWG climatology to the RCMs and their boundary conditions is further demonstrated in Figure 8. The spatial distributions of mean DPWG are plotted for RCA4 and RACMO22E driven by three boundary conditions (i.e., ERAINT, ICHEC and MOHC). The spatial patterns of DPWG do not vary much when the same RCM is integrated with different boundary conditions. A large discrepancy is instead found between the two RCMs regardless of boundary conditions. Specifically, RCA4 shows a larger west-east or north-south contrast in DPWG than RACMO22E.

5.3. Observations Versus Simulations

Figure 9 shows the seasonal cycle of the observed and modeled mean DPWG during 1996–2005 for coastal, inland, and mountain regions. The seasonal cycle is displayed as a station/grid box series ensemble (together with the ensemble mean for each dataset), i.e. the ensemble range spans from the maximum to the minimum average DPWG value recorded for each month by the station series (or closest grid box series for RCMs) belonging to that region. In coastal regions, although slightly overestimated, all RCM simulations successfully reproduce the observed seasonal cycle with a stronger DPWG during winter than during summer. Across inland and mountain regions, the two RCMs exhibit subtle differences. The RCA4 shows a stronger seasonality than the RACMO22E. This model particularly simulates a stronger DPWG during colder seasons at inland stations, although the observations do not show a pronounced seasonality. A similar underestimation is found in mountain regions during summer. The RACMO22E exhibits a weak seasonality of DPWG across both inland and mountain stations. This model tends to overestimate inland DWPG, but underestimate mountain DWPG. This causes no difference in annual-mean DWPG between inland and mountain regions. Notice that, similar to what was shown in Figures 5 and 6, ERAINT cannot capture the difference in seasonal cycle between inland and mountain stations.

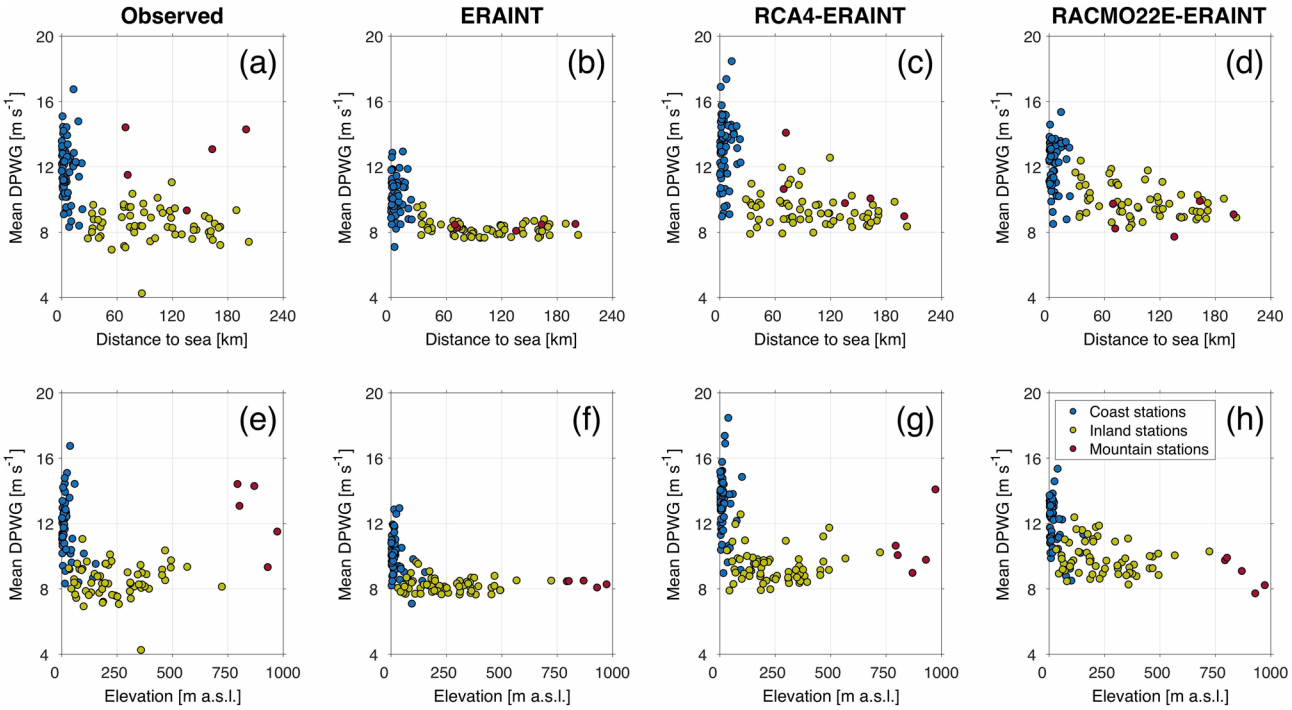

Figure 6. Scatterplot of the 1996–2005 mean of daily peak wind gusts (DPWG) for the 127 stations across Scandinavia plotted against station distance to the sea (top row) and elevation (bottom row) calculated using (from right to left) the observed, ERAINT, RCA4-ERAINT and RACMO22E series. Scatter-points are filled according to their region: (i) coast (sky-blue), (ii) inland (olive) and (iii) mountain (brown).

The performances of RCMs are further demonstrated in Figure 10, where the box-and-whisker plots of observed and simulated DPWG are compared during 1996–2005. In coastal areas, all RACMO22E datasets agrees well with the observations, while the RCA4 overestimate the observed distribution with a large variability between the stations. For inland stations, the box-and-whisker plots of all the datasets are pretty similar to the observed statistics. Instead, all RCMs show limitations in mountain regions, where the distribution of observed DPWG does not resemble the simulated ones.

Overall, the analyzed RCMs were able to reasonably well simulate the DPWG statistics across both coastal and inland regions. However, in the mountainous regions where surface forcing (and subgrid scale processes parametrization) are strongly affected by the complex topography, all the RCMs struggled to capture the observed DPWG characteristics.

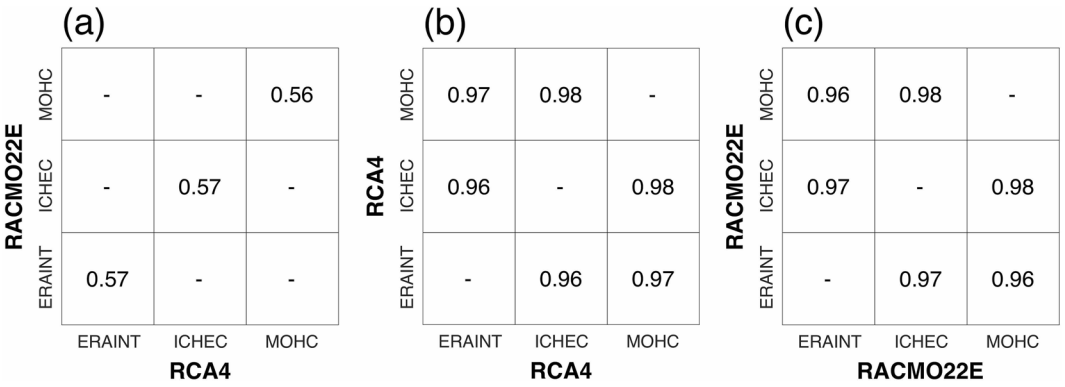

Figure 7. Comparison of the R^2 values for the scatterplot of 1996–2005 mean daily peak wind gusts between RCMs (RCA4 and RACMO22E) having same driving models (left) and between the same RCM (RCA4 in the middle and RACMO22E to the right) with different driving models (ERAINT, ICHEC and MOHC).

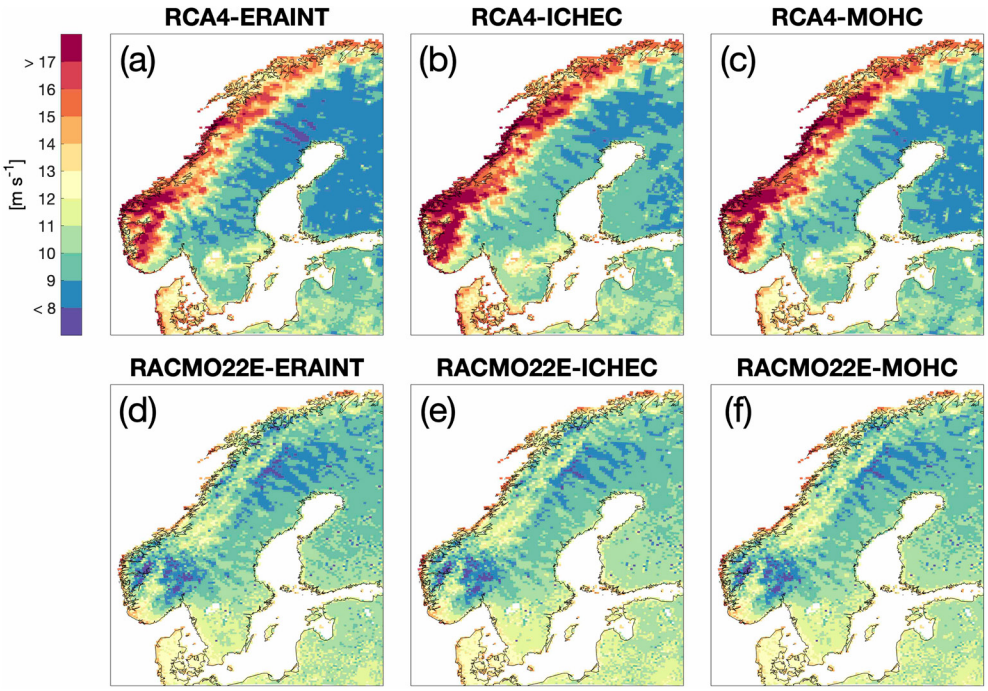

Figure 8. Spatial distribution of the annual 1996–2005 mean daily peak wind gusts for the RCA4 (top row) and RACMO22E (bottom row) datasets with the ERAINT (left), ICHEC (middle) and MOHC (right) driving models.

6. Discussion

This study created the longest available (1996–2016) dataset of homogeneous and complete DPWG observations across Scandinavia. The dataset is analyzed here for the first time. According to the observed DPWG climate statistics, three regions can be identified: (i) coastal stations, (ii) inland stations and (iii) mountain stations with higher elevations. The rapid change in DPWG strength from the coast toward inland regions has already been reported in near-surface wind speeds across Sweden by Achberger et al. (2006) and Minola et al. (2016). Here, wind statistics are characterized by the strong, large-scale westerly winds and synoptic flows associated with extratropical cyclones, which are particularly dominant during winter months (Achberger et al., 2006; Feser et al., 2015).

In model simulations, land-sea roughness and temperature differences along the coastline were captured by both the RCMs and driving models, where those large-scale features, together with the large-scale flows, were included. Local wind circulations, which can arise from the complex topography and could be missed in the models, are often obscured by winds associated with synoptic-scale weather systems (Borne et al., 1998). Over land, where surface forcing plays a key role, topography is crucial when considering differences in DPWG climate statistics across stations with varying elevations. For example, over complex topographic regions, large-scale wind circulation is broken by localized circulations driven by valleys and mountains (Helbig et al., 2017; Rotach et al., 2015; Serafin et al., 2018). A similar topographic influence has been reported for the precipitation distribution across Sweden by Johansson and Chen (2003). On the basis of these observations, differences in DPWG between inland and mountain regions can be discerned only when topographic features are included. Unfortunately, the coarse spatial resolution of the driving models (e.g., ERAINT, ~80 km) cannot resolve those complex terrain features, thereby hindering the simulation of DPWG characteristics across Scandinavia. In contrast, RCMs have a greater horizontal resolution and were able to capture the differences between the three observed DPWG regions, demonstrating added value in simulating DPWG when compared to their driving models. This justifies the use of RCM downscaling for DPWG studies across Scandinavia, as considered by Kjellström et al. (2005), Rockel and Woth (2007), Nikulin et al. (2010) and Strandberg et al. (2014).

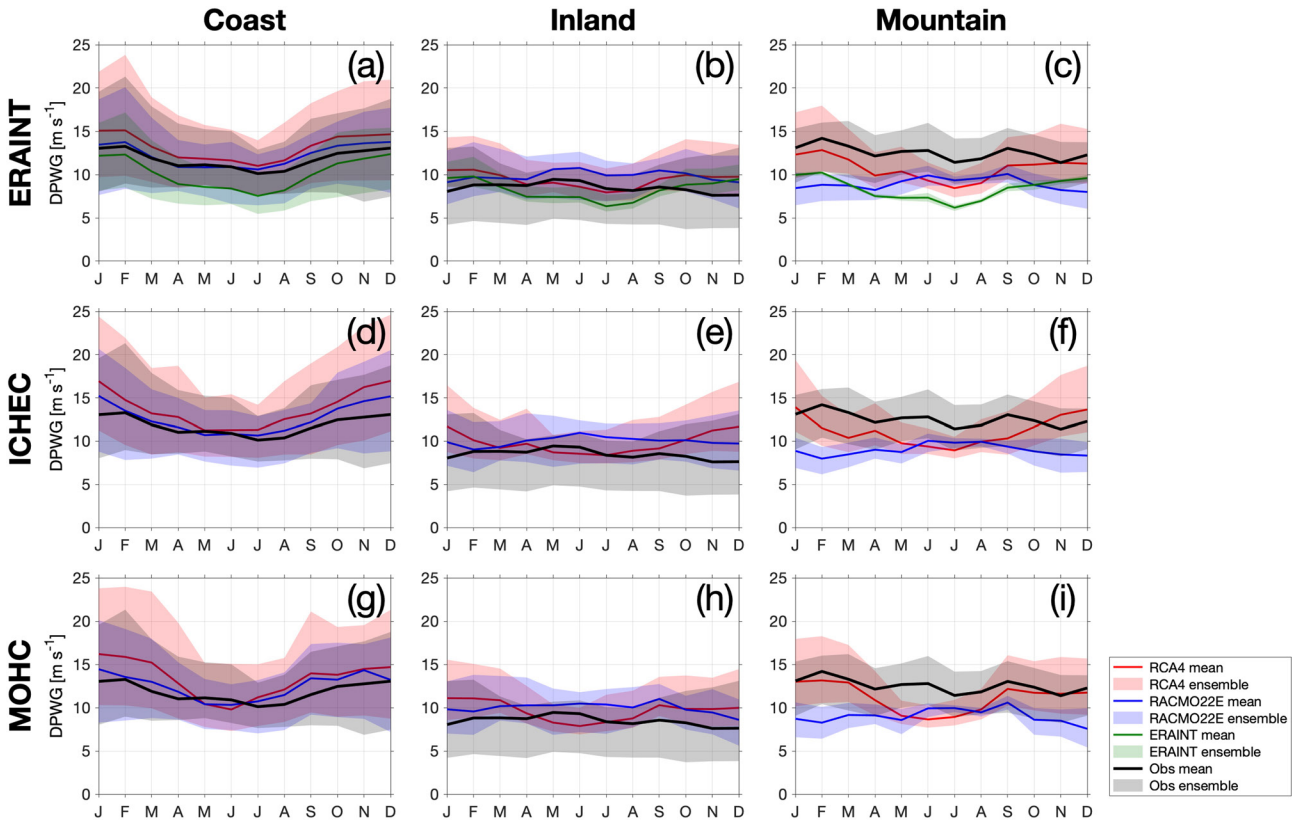

Figure 9. Mean seasonal cycle of daily peak wind gusts (DPWG) series calculated using observations (black), ERAINT (green), RCA4 (red) and RACMO22E (blue) with different driving models (ERAINT, top row; ICHEC, middle row; MOHC, bottom row) in coastal (left), inland (middle) and mountain (right) regions for 1996–2005. The seasonal cycle is displayed as the mean (solid line) and the ensemble range (colored area) of the seasonal variability for the different series in the same dataset.

The use of a consistent set of boundary conditions for both RCMs selected here provides the opportunity to study the role of RCM configuration in the simulated climatology distribution under the same large-scale forcing. When looking at climate averages (e.g., mean seasonal cycle and geographical distribution of means and standard deviations), the performances of RCMs in simulating DPWG are more sensitive to the dynamics and physics (e.g., parametrization) of the model than to the adopted boundary conditions. Instead, the role of boundary forcing becomes relevant when looking at climate variability and changes (e.g., long-term trends; Déqué et al., 2007).

Overall, both RCMs performed well in simulating observed DPWG across coastal regions. In inland areas, they still closely resembled the climate statistics, but differences became more noticeable (e.g., strong RCA4 seasonality vs. weak observed seasonality). Across mountainous regions, all RCMs struggle to simulate the observed DPWG features, although the mismatch in RACMO22E is mostly caused by a negative bias. Results shows that the two RCMs can not adequately simulate the inland and mountain wind climate, where surface forcing and subgrid scale parametrizations play a key role (Kunz et al., 2010). This calls for an even higher resolution, where downscaling can capture the complex topographic influences, and/or better representation of relevant physical processes. As shown by Kunz et al. (2010), moving from 18- to 10-km spatial resolution improves the simulated spatial variability of gusts over complex terrain. However, for a reliable representation of local wind extremes, even higher resolution is needed. Based on these requirements, a promising framework for improved DPWG simulations at regional to local scales can be provided by RCMs using convection-permitting models (CPMs), with a horizontal grid spacing ~4 km (Kendon et al., 2017; Prein et al., 2015). Even though CPM simulations cannot be the cure for all model biases, they have the advantage of explicitly resolving deep convection (e.g., frontal situations and mid-latitude summer convective systems; Bechtold & Bidlot, 2009; Punkka & Bister, 2015), avoiding error-prone convection parametrizations

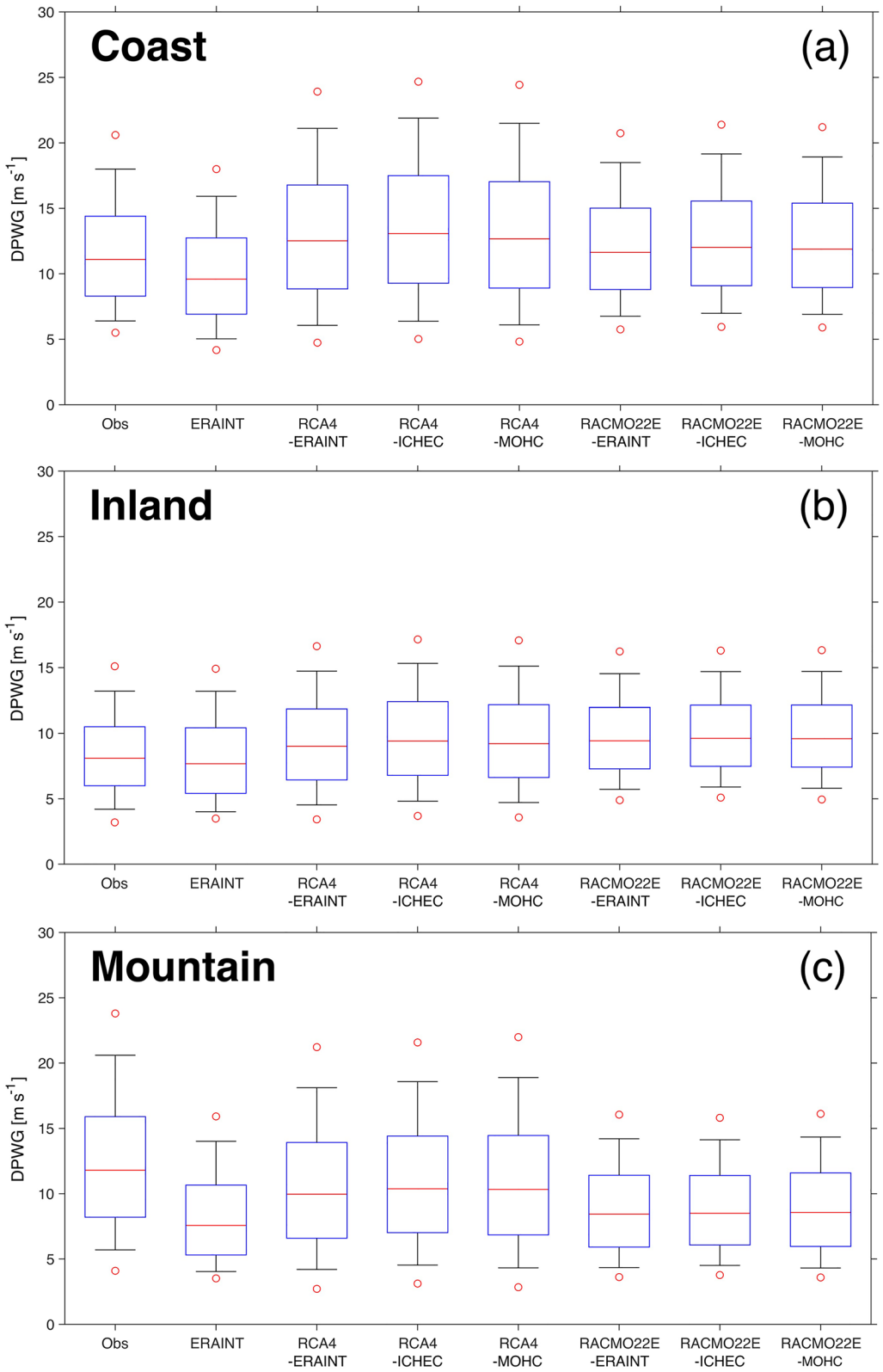

Figure 10. Box-and-whisker plots of daily peak wind gusts (DPWG) for 1996–2005 series classified as coastal (top), inland (middle) and mountain (bottom) stations in different datasets (observations, ERAINT, RCA4 and RACMO22E with different driving models - ERAINT, ICHEC, MOHC). The median (red line), the 25th and 75th percentile range (bottom and top edges of the blue box), the 10th and 90th percentiles (whiskers), and the 5th and 95th percentiles (red circles) are represented.

and better resolving topographic and surface forcing in regions with strong spatial heterogeneities (e.g., mountain areas). Future studies should explore the possibility of using CPMs to simulate wind gustiness across Scandinavia, following Pantillon et al. (2018) where the predictability of wind gusts during winter storms was investigated in an ensemble prediction system running at convection-permitting resolution.

In general, the two analyzed RCMs perform differently in all the regions (e.g., RACMO22E outperforms RCA4 in coastal regions, whereas RCA4 is better over the mountain areas; both models have similar statistics in the inland area). This study did not address the underlying reason of their different performance. Although RCA4 and RACMO22E use different gust parametrizations, this is only one of the factors that may affect the differences in their ability to simulate DPWG. Under the same boundary conditions, model differences also arise from the different techniques used to discretize the equations and to represent other subgrid effects, such as the planetary boundary layer (PBL) parametrization (Déqué et al., 2007). To isolate the impact of the gust parametrization, future studies should run the same model (where model physics is kept unchanged) with different gust parameterizations, following Kurbatova et al. (2018). This could provide further insights into how DPWG simulations could be improved.

7. Conclusions

To summarize, the main findings of this study are:

- DPWG series from 127 stations in Finland, Norway and Sweden are collected and homogenized to create the first and longest available (1996–2016) DPWG dataset across Scandinavia.
- Geographic settings of a station are important factors underlying differences in DPWG climate features, and it is useful to classify the observation stations into three groups: coast, inland and mountain.
- RCM downscaling is needed to distinguish between the three groups and to achieve more realistic DPWG simulations when compared to their driving models, in regions where the more complex topography cannot be adequately resolved.
- The two selected RCMs are able to model DPWG conditions along the coastline, but show poor skill in simulating the inland and mountain wind climate. The model performance is sensitive not to the choice of boundary conditions but to the choice of model. This calls for an even higher resolution and better representation of relevant physical processes in RCMs.

Data Availability Statement

The homogenized DPWG series can be downloaded through the following link: https://figshare.com/articles/dataset/Daily_Peak_Wind_Gust_series/14152529 (last accessed February 16, 2021).

Acknowledgments
This study contributes to the strategic research areas of Modeling the Regional and Global Earth system (MERGE) and Biodiversity and Ecosystem services in a Changing Climate (BECC). It is supported by Swedish Research Council (2017-03780) and Spanish Ministry of Science, Innovation and Universities (RTI2018-095749-A-I00). C. Azorin-Molina was supported by the Ramon y Cajal fellowship (RYC-2017-22,830). G. F. Zhang was supported by the Second Tibetan Plateau Scientific Expedition and Research Program (STEP-2019QZ-KK0606) and the National Natural Science Foundation of China (41621061). S. W. Son was supported by the National Foundation of Korea (NFR) grant funded by the Korean government (MSIT) (NFR2018R1A5A1024958). The authors would like to thank FMI, MET Norway and SMHI for providing wind gust measurements; and SMHI for the access to the climate model simulations from the CORDEX project. The authors would also like to thank ECMWF for the access to ERAINT outputs. The authors wish to thank Sofie Lekander from SMHI customer service, Reidun G. Skaland and Hilsen T. Husebye from MET Norway and Juho-Pekka Kaukoranta and Maria Santanen from FMI, who supplied important information about how wind is measured in Sweden, Norway and Finland, respectively. The authors would like to thank Grigory Nikulin from SMHI for the info regarding the RCA4 design. The authors are grateful to the three anonymous reviewers for their constructive and helpful comments to the original manuscript.

References

Achberger, C., Chen, D., & Alexandersson, H. (2006). The surface winds of Sweden during 1999–2000. *International Journal of Climatology*, *26*, 159–178. https://doi.org/10.1002/joc.1254

Aguilar, E., Auer, I., Brunet, M., Peterson, T. C., & Wieringa, J. (2003). *Guidelines on climate metadata and homogenization* (Technical Document No. 1186). WMO. Retrieved from https://library.wmo.int/index.php?lvl=notice_display&id=11635#.XmqUtlAo8dV

Alexandersson, H. (1986). A homogeneity test applied to precipitation data. *Journal of Climatology*, *6*, 661–675. https://doi.org/10.1002/joc.3370060607

Anthes, R. A. (1985). *Introduction to parametrization of physical processes in numerical models. Paper presented at the seminar on physical parametrization for numerical models of the atmosphere*. Shinfield Park, Reading, UK:ECMWF. Retrieved from https://www.ecmwf.int/en/elibrary/7786-introduction-parameterization-physical-processes-numerical-models

Azorin-Molina, C., Asin, J., McVicar, T. R., Minola, L., Lopez-Moreno, J. I., Vicente-Serrano, S. M., & Chen, D. (2018a). Evaluating anemometer drift: A statistical approach to correct biases in wind speed measurement. *Atmospheric Research*, *203*, 175–188. https://doi.org/10.1016/j.atmosres.2017.12.010

Azorin-Molina, C., Guijarro, J. A., McVicar, T. R., Trewin, B. C., Frost, A. J., & Chen, D. (2019). An approach to homogenize daily peak wind gusts: An application to the Australian series. *International Journal of Climatology*, *39*, 2260–2277. https://doi.org/10.1002/joc.5949

Azorin-Molina, C., Guijarro, J.-A., McVicar, T. R., Vicente-Serrano, S. M., Chen, D., Jerez, S., & Espírito-Santo, F. (2016). Trends of daily peak wind gusts in Spain and Portugal, 1961–2014. *Journal of Geophysical Research: Atmospheres*, *121*, 1059–1078. https://doi.org/10.1002/2015JD024485

Azorin-Molina, C., Rehman, S., Guijarro, J. A., McVicar, T. R., Minola, L., Chen, D., & Vicente-Serrano, S. M. (2018b). Recent trends in wind speed across Saudi Arabia, 1978–2013: A break in the stilling. *International Journal of Climatology*, *38*(Suppl. 1), e966–e984. https://doi.org/10.1002/joc.5423

Bechtold, P., & Bidlot, J.-R. (2009). Parametrization of convective gusts. *ECMWF Newsletter*, *199*, 15–18. https://doi.org/10.21957/kfr42kfp8c

Beniston, M., Stephenson, D. B., Christensen, O. B., Ferro, C. A. T., Frei, C., Goyette, S., et al. (2007). Future extreme events in European climate: An exploration of regional climate model projections. *Climatic Change*, *81*, 71–95. https://doi.org/10.1007/s10584-006-9226-z

Borne, K., Chen, D., & Nunez, M. (1998). A method for finding sea breeze days under stable synoptic conditions and its application to the Swedish west coast. *International Journal of Climatology*, *18*, 901–914. https://doi.org/10.1002/(SICI)1097-0088(19980630)18:8<901::AID-JOC295>3.0.CO;2-F

Brasseur, O. (2001). Development and application of a physical approach to estimating wind gusts. *Monthly Weather Review*, *129*, 5–25. https://doi.org/10.1175/1520-0493(2001)129<0005:DAAOAP>2.0.CO;2

Chen, D., Rodhe, H., Emanuel, K., Seneviratne, I., Zhai, P., Allard, B., et al. (2020). Summary of a workshop on extreme weather events in a warming world organized by the Royal Swedish Academy of Sciences. *Tellus*, *72*, 1794236. https://doi.org/10.1080/16000889.2020.1794236

Dee, D. P., Uppala, S. M., Simmons, A. J., Berrisford, P., Poli, P., Kobayashi, S., et al. (2011). The ERA-Interim reanalysis: Configuration and performance of the data assimilation system. *Quarterly Journal of the Royal Meteorological Society*, *137*, 553–597. https://doi.org/10.1002/qj.828

Déqué, M., Rowell, D. P., Lüthi, D., Giorgi, F., Christensen, J. H., Rockel, B., et al. (2007). An intercomparison of regional climate simulations for Europe: Assessing uncertainties in model projections. *Climatic Change*, *81*, 53–70. https://doi.org/10.1007/s10584-006-9228-x

European Center for Medium-Range Weather Forecasts (ECMWF). (2007). IFS documentation CY31R1—Part IV: Physical processes. IFS documentation. Retrieved from https://www.ecmwf.int/en/elibrary/9221-part-iv-physical-processes

European Environmental Agency (EEA) (2019). *Economic losses from climate-related extremes in Europe*. Copenhagen, Denmark: EEA. Retrieved from https://www.eea.europa.eu/data-and-maps/indicators/direct-losses-from-weather-disasters-3/assessment-2

Feser, F., Barcikowska, M., Krueger, O., Schenk, F., Weisse, R., & Xia, L. (2015). Storminess over the North Atlantic and northwestern Europe—A review. *Quarterly Journal of the Royal Meteorological Society*, *141*, 350–382. https://doi.org/10.1002/qj.2364

Giorgi, F., Jones, C., & Asrar, G. R. (2009). *Addressing climate information needs at the regional level: The CORDEX framework*. WMO Bulletin. Retrieved from https://public.wmo.int/en/bulletin/addressing-climate-information-needs-regional-level-cordex-framework

Gregow, H., Laaksonen, A., & Alper, M. (2017). Increasing large scale windstorms damage in Western, Central and Northern European forests, 1951–2010. *Scientific Reports*, *7*, 46397. https://doi.org/10.1038/srep46397

Guijarro, J. A. (2017). Daily series homogenization and gridding with Climatol v.3. In *Ninth seminar for homogenization and quality control in climatological databases and fourth conference on spatial interpolation techniques in climatology and meteorology* (pp. 175–180). Budapest, Hungary: WMO. Retrieved from https://library.wmo.int/doc_num.php?explnum_id=5680

Guijarro, J. A. (2018). *Homogenization of climate series with Climatol*. Retrieved from http://www.climatol.eu/homog_climatol-en.pdf

Hannon Bradshaw, L. (2017). *Sweden, forests & wind storms: Developing a model to predict storm damage to forests in Kronoberg county (Master's thesis)*. Lund, Sweden: Lund University Publications Student Papers, Department of Physical Geography and Ecosystem Science. Retrieved from https://lup.lub.lu.se/student-papers/search/publication/8908951

Helbig, N., Mott, R., van Herwijnen, A., Winstral, A., & Jonas, T. (2017). Parameterizing surface wind speed over complex topography. *Journal of Geophysical Research: Atmospheres*, *122*, 651–667. https://doi.org/10.1002/2016JD025593

Intergovernmental Panel on Climate Change (IPCC). (2014). *Climate change 2014: Synthesis report*. Geneva, Switzerland: IPCC. Retrieved from https://www.ipcc.ch/report/ar5/syr/

Jeong, D. I., & Sushama, L. (2019). Projected changes to mean and extreme surface wind speeds for North America based on regional climate model simulations. *Atmosphere*, *10*, 497. https://doi.org/10.3390/atmos10090497

Johansson, B., & Chen, D. (2003). The influence of wind and topography on precipitation distribution in Sweden: Statistical analysis and modelling. *International Journal of Climatology*, *23*, 1523–1535. https://doi.org/10.1002/joc.951

Kendon, E. J., Ban, N., Roberts, N. M., Fowler, H. J., Roberts, M. J., Chan, S. C., et al. (2017). Do convection-permitting regional climate models improve projections of future precipitation change? *Bulletin of the American Meteorological Society*, *98*, 79–93. https://doi.org/10.1175/BAMS-D-15-0004.1

Kjellström, E., Bärring, L., Gollvik, S., Hansson, U., Jones, C., Samuelsson, P., et al. (2005). A 140-year simulation of European climate with the new version of the Rossby Centre regional atmospheric climate model (RCA3). SMHI Reports Meteorology and Climatology (No. 108). Norrköping, Sweden: SMHI. Retrieved from https://www.smhi.se/polopoly_fs/1.2104!/RMK108%5B1%5D.pdf

Kotlarski, S., Keuler, K., Christensen, O. B., Colette, A., Déqué, M., Gobiet, A., et al. 2014). Regional climate modeling on European scales: A joint standard evaluation of the EURO-CORDEX RCM ensemble. *Geoscientific Model Development*, *7*, 1297–1333. https://doi.org/10.5194/gmd-7-1297-2014

Kunz, M., Mohr, S., Rauthe, M., Lux, R., & Kottmeier, C. (2010). Assessment of extreme wind speeds from regional climate models—Part 1: Estimation of return values and their evaluation. *Natural Hazards and Earth System Sciences*, *10*, 907–922. https://doi.org/10.5194/nhess-10-907-2010

Kurbatova, M., Rubinstein, K., Gubenko, I., & Kurbatov, G. (2018). Comparison of seven wind gust parameterizations over the European part of Russia. *Advances in Science and Research*, *15*, 251–255. https://doi.org/10.5194/asr-15-251-2018

Lenaerts, J. T. M., Smeets, C. J. P. P., Nishimura, K., Eijkelboom, M., Boot, W., van den Broeke, M. R., & van de Berg, W. J. (2014). Drifting snow measurements on the Greenland Ice Sheet and their application for model evaluation. *The Cryosphere*, *8*, 801–814. https://doi.org/10.5194/tc-8-801-2014

Minola, L., Azorin-Molina, C., & Chen, D. (2016). Homogenization and assessment of observed near-surface wind speed trends across Sweden, 1956–2013. *Journal of Climate*, *29*, 7397–7415. https://doi.org/10.1175/JCLI-D-15-0636.1

Minola, L., Zhang, F., Azorin-Molina, C., Safaei Pirooz, A. A., Flay, R. G. J., Hersbach, H., & Chen, D. (2020). Near-surface mean and gust wind speeds in ERA5 across Sweden: Towards an improved gust parametrization. *Climate Dynamics*, *55*, 887–907. https://doi.org/10.1007/s00382-020-05302-6

Nikulin, G., Kjellström, E., Hansson, U., Strandberg, G., & Ullerstig, A. (2010). Evaluation and future projections of temperature, precipitation and wind extremes over Europe in an ensemble of regional climate simulations. *Tellus A*, *63*, 41–55. https://doi.org/10.1111/j.1600-0870.2010.00466.x

Panofsky, H. A., Tennekes, H., Lenschow, D. H., & Wyngaard, J. C. (1977). The characteristics of turbulent velocity components in the surface layer under convective conditions. *Boundary-Layer Meteorology*, *11*(3), 355–361. https://doi.org/10.1007/BF02186086

Pantillon, F., Lerch, S., Knippertz, P., & Corsmeier, U. (2018). Forecasting wind gusts in winter storms using a calibrated convection-permitting ensemble. *Quarterly Journal of the Royal Meteorological Society*, *144*, 1864–1881. https://doi.org/10.1002/qj.3380

Peltola, H., Ikonen, V.-P., Gregow, H., Strandman, H., Kilpeläinen, A., Venäläinen, A., & Kellomäki, S. (2010). Impacts of climate change on timber production and regional risks of wind-induced damage to forests in Finland. *Forest Ecology and Management*, *260*, 833–845. https://doi.org/10.1016/j.foreco.2010.06.001

Prein, A. F., Langhans, W., Fosser, G., Ferrone, A., Ban, N., Goergen, K., et al. (2015). A review on regional convection-permitting climate modeling: Demonstrations, prospects, and challenges. *Reviews of Geophysics*, *53*, 323–361. https://doi.org/10.1002/2014RG000475

Punkka, A.-J., & Bister, M. (2015). Mesoscale convective systems and their synoptic-scale environment in Finland. *Weather and Forecasting*, *30*, 182–196. https://doi.org/10.1175/WAF-D-13-00146.1

Räisänen, J., Hansson, U., Ullerstig, A., Döscher, R., Graham, L. P., Jones, C., et al. (2003). GCM driven simulations of recent and future climate with the Rossby Centre coupled atmosphere—Baltic Sea regional climate model RCA0. Reports Meteorology and Climatology (No. 101). Norrköping, Sweden: SMHI. Retrieved from https://www.smhi.se/polopoly_fs/1.19050!/RMK101.pdf

R Core Team. (2020). *R: A language and environment for statistical computing*. Vienna, Austria: R Foundation for Statistical Computing. Retrieved from https://cran.r-project.org/doc/manuals/r-release/fullrefman.pdf

Rockel, B., & Woth, K. (2007). Extremes of near-surface wind speed over Europe and their future changes as estimated from an ensemble of RCM simulations. *Climatic Change*, *81*, 267–280. https://doi.org/10.1007/s10584-006-9227-y

Rotach, M. W., Gohm, A., Lang, M. N., Leukauf, D., Stiperski, I., & Wagner, J. S. (2015). On the vertical exchange of heat, mass, and momentum over complex, mountainous terrain. *Frontiers in Earth Science*, *3*, 76. https://doi.org/10.3389/feart.2015.00076

Samuelsson, P., Gollvik, S., Jansson, C., Kupiainen, M., Kourzeneva, E., & van de Berg, W. J. (2015). *The surface processes of the Rossby Centre regional atmospheric climate model (RCA4). Meteorologi (Nr 157)*. Norrköping, Sweden: SMHI. Retrieved from http://www.smhi.se/polopoly_fs/1.89799!/Menu/general/extGroup/attachmentColHold/mainCol1/file/meteorologi_157.pdf

Serafin, S., Adler, B., Cuxart, J., De Wekker, S., Gohm, A., Grisogono, B., et al. (2018). Exchange processes in the atmospheric boundary layer over mountainous terrain. *Atmosphere*, *9*, 102. https://doi.org/10.3390/atmos9030102

Sheridan, P. (2011). *Review of techniques and research for gust forecasting and parametrization (Forecasting Research Technical Report 570)*. Exeter, UK: Met Office.

Shi, P., Zhang, G., Kong, F., Chen, D., Azorin-Molina, C., & Guijarro, J. A. (2019). Variability of winter haze over the Beijing-Tianjin-Hebei region tied to wind speed in the lower troposphere and particulate sources. *Atmospheric Research*, *215*, 1–11. https://doi.org/10.1016/j.atmosres.2018.08.013

Strandberg, G., Bärring, L, Hansson, U., Jansson, C., Jones, C., Kjellström, E., et al. (2014). *CORDEX scenarios for Europe from the Rossby Centre regional climate model RCA4. SMHI Reports Meteorology and Climatology (No. 116)*. Norrköping, Sweden: SMHI. Retrieved from https://www.smhi.se/polopoly_fs/1.90273!/Menu/general/extGroup/attachmentColHold/mainCol1/file/RMK_116.pdf

Suomi, I., & Vihma, T. (2018). Wind gust measurement techniques-from traditional anemometry to new possibilities. *Sensors*, *18*, 1300. https://doi.org/10.3390/s18041300

Taylor, K. E., Stouffer, R. J., & Meehl, G. A. (2012). An overview of CMIP5 and the experiment design. *Bulletin of the American Meteorological Society*, *93*, 485–498. https://doi.org/10.1175/BAMS-D-11-00094.1

Ulbrich, U., Leckebush, G. C., & Donat, M. G. (2013). Windstorms, the most costly natural hazard in Europe. In S. Boulter, J. Palutikof, D. Karoly, D. Guitart (Eds.), *Natural disasters and adaptation to climate change* (pp. 109–120), Cambridge, UK: Cambridge University Press.

Undén, P., Rontu, L., Järvinen, H., Lynch, P., Calco, J., Cats, G., et al. (2002). *HIRLAM-5 scientific report* (Technical Report). Norrköping, Sweden: SMHI. Retrieved from http://www.hirlam.org/index.php/hirlam-documentation/cat_view/114-model-and-system-documentation/131-hirlam-documentation?limit=5&order=date&dir=ASC&start=10

van Meijgaard, E., van Ulft, L. H., Lenderink, G., de Roode, S. R., Wipfler, L., Boers, R., & Timmermans, R. M. A. (2012). *Refinement and application of a regional atmospheric model for climate scenario calculations of Western Europe (KVR Rep. No. 054/12)*. Wageningen, Netherlands: KNMI. Retrieved from https://library.wur.nl/WebQuery/wurpubs/fulltext/312258

Von Storch, H., & Zwiers, F. W. (1999). *Statistical analysis in climate research*, Cambridge, UK: Cambridge University Press.

Wan, H., Wang, X. L., & Swail, V. R. (2010). Homogenization and trend analysis of Canadian near-surface wind speeds. *Journal of Climate*, *23*, 1209–1225. http://doi.org/10.1175/2009JCLI3200.1

Wern, L., & Bärring, L. (2009). *Sveriges vindklimat 1901–2008: Analys av trend i geostrofisk vind. Meteorologi (Nr 138)*. Norrköping, Sweden: SMHI. Retrieved from http://www.smhi.se/polopoly_fs/1.7843!/meteorologi_138.pdf

World Meteorological Organization (WMO). (1987). *The measurement of gustiness at routine wind stations—A review*. Instruments and Observing Methods (Rep. No. 31). Retrieved from https://library.wmo.int/doc_num.php?explnum_id=7372

World Meteorological Organization (WMO). (2014). *Guide to meteorological instruments and methods of observations* (WMO-No. 8). Geneva, Switzerland: WMO. Retrieved from https://library.wmo.int/doc_num.php?explnum_id=4147

Zhang, G., Azorin-Molina, C., Chen, D., Guijarro, J. A., Kong, F., Minola, L., et al. (2020). Variability of daily maximum wind speed across China, 1975–2016: An examination of likely causes. *Journal of Climate*, *33*, 2793–2816. https://doi.org/10.1175/JCLI-D-19-0603.s1

Zheng, Z., Ziegler, A. D., Searchinger, T., Yang, L., Chen, A., Ju, K., et al. (2019). A reversal in global terrestrial stilling and its implications for wind energy production. *Nature Climate Change*, *9*, 979–985. https://doi.org/10.1038/s41558-019-0622-6